UCRL-16127

University of California

Ernest O. Lawrence Radiation Laboratory

TWO-WEEK LOAN COPY

This is a Library Circulating Copy which may be borrowed for two weeks. For a personal retention copy, call Tech. Info. Division, Ext. 5545

TECHNIQUES FOR MEASURING STRESS-STRAIN RELATIONS AT HIGH STRAIN RATES

Berkeley, California

DISCLAIMER

This document was prepared as an account of work sponsored by the United States Government. While this document is believed to contain correct information, neither the United States Government nor any agency thereof, nor the Regents of the University of California, nor any of their employees, makes any warranty, express or implied, or assumes any legal responsibility for the accuracy, completeness, or usefulness of any information, apparatus, product, or process disclosed, or represents that its use would not infringe privately owned rights. Reference herein to any specific commercial product, process, or service by its trade name, trademark, manufacturer, or otherwise, does not necessarily constitute or imply its endorsement, recommendation, or favoring by the United States Government or any agency thereof, or the Regents of the University of California. The views and opinions of authors expressed herein do not necessarily state or reflect those of the United States Government or any agency thereof or the Regents of the University of California.

Journal of the Society for Experimental Stress Analysis

UCRL-16127

UNIVERSITY OF CALIFORNIA

Lawrence Radiation Laboratory
Berkeley, California

AEC Contract W-7405-eng-48

TECHNIQUES FOR MEASURING STRESS-STRAIN RELATIONS AT HIGH STRAIN RATES

Frank E. Hauser

March 1965

ABSTRACT

The qualitative dependence of the mechanical behavior of some materials on strain rate is now well known. But the quantitative relation between stress, strain and strain rate has been established for only a few materials and for only a limited range. This relation, the so called constitutive equation, must be known before plasticity or plastic wave propagation theory can be used to predict the stress or strain distribution in parts subjected to impact stresses above the yield strength.

In this paper a brief review of some of the experimental techniques for measuring the stress, strain, strain rate relationship is given and some of the difficulties and shortcomings pointed out. Ordinary creep or tensile tests can be used at plastic strain rates from 10^{-8} to about 10^{-1} per second. Special quasi-static tests in which the stress and strain measuring devices as well as the specimen geometry and support have been optimized are capable of giving accurate results to strain rates of about 10^{2} per second. At higher strain rates it is shown that wave propagation effects must be included in the design and analysis of the experiments. Special testing machines for measuring stress, strain, strain rate relationships in compression, tension and shear at strain rates up to 10^{5} per second are described and some of the results presented. With this type of testing machine the analysis of the data requires certain assumptions whose validity depends upon proper design of the equipment. A critical evaluation of the accuracy in these types of tests is presented.

INTRODUCTION

The mechanical behavior of most materials is known to be influenced greatly by the testing temperature and to a somewhat less degree by the rate of deformation. The many studies of the temperature effect have helped not only the engineer in designing structures at temperature extremes, but also the scientist in the understanding of the basic plastic deformation mechanisms. Only more recently have accurate studies of the rate effect over wide ranges of strain rate become possible and these results have been valuable to check proposed rate determining plastic deformation mechanisms. The necessity of knowing the effect of rate on the behavior of materials is not only necessary to scientific endeavors but also to practical engineering considerations when designing members which are subjected to impacts. Thus under the combined pressure of scientific as well as practical investigations of the rate effect, many schemes have been devised to measure the stress, strain and strain rate over wide ranges of strain rate.

J. M. Krafft[1] and H. Kolsky[2] have given excellent reviews of some of the earlier schemes of measuring high strain rates. In prior publications on strain rate effects by the author[3,4,5] the emphasis has been on the material properties and the experimental techniques for measuring these properties were not included. In this paper, after a brief section on the derivation of pertinent equations, the experimental techniques used by the author will be explained and typical results presented.

In a simple tension test such as Fig. 1a the load and the initial specimen area are known and thus the engineering stress readily defined.

Also the initial gage length and change in length as a function of time can be measured and the engineering strain and strain rate calculated. Then, if one assumes uniform strain distribution throughout the gage section, the true stress and strain can be calculated. But if localized deformation such as a Luders band or necking occur, the local stress and strain can only be obtained by measuring the elongation in the small region where these strains can again be assumed to be uniform. Similarly if the rate of loading is increased greatly, at any instant of time the load reading at the load cell may be different from the load carried by the specimen and the strain distribution within the gage length may vary considerably due to the finite rate of stress and strain propagation. To obtain useful data at high strain rates the load cell must be small and be in intimate contact with the specimen and the specimen itself must be very small in order to approach uniform strain distribution in a short time. This is the quasi-static testing approach shown in Fig. 1b. It assumes that the upper and lower loading members approach each other at a known velocity and are essentially infinite in size. If these loading members have changes in cross section, elastic stress waves within the members will be reflected from these discontinuities and cause a peculiar stepwise loading rate. To avoid this difficulty one can use long slender elastic input and output bars such as in Fig. 1c in which the theoretical solutions to wave propagation equations are relatively simple and so the stress variation can be predicted and controlled. In Fig. 1c, on impact of the ram with the input bar a stress wave propagates down the bar past strain gage A where the magnitude can be measured. On reaching the specimen, part of the wave is transmitted through the specimen and part is

reflected back toward the ram. The magnitude of the reflected wave can be measured again at gage A and the stress transmitted through the specimen can be measured in the output bar with gage B. Eventually the compressive stress wave is reflected from the free end as a tension wave and arrives back at the specimen. This unloading wave terminates the test. If properly analyzed, enough data is available from the strain gages to determine the stress, strain, strain rate of the material in the specimen. The analysis of the data and the optimization of the experiment requires some background in simple wave propagation theory. A review of the pertinent part of the theory follows.

ELASTIC WAVE PROPAGATION AT DISCONTINUITIES

Fig. 2 derives the pertinent equations describing the reflected stress σ_r and the transmitted stress σ_t in terms of the incoming stress wave σ_i and the areas A_1, A_2 and mass densities ρ_1, ρ_2. This derivation assumes uniaxial stress and thus holds only for slender bars. Fig. 3 shows the repeated applications of equations (4) and (5) to an example where a 1" long reduced section of $\frac{1}{2}$ the area of the input and output rod is inserted. The incoming stress wave σ_i has a rise time of 2 μsec. Note that the stress in bar 1 first rises to σ_i, then drops due to the reflection from the discontinuity and then rises again stepwise at 10 μsec. intervals assymptotically toward σ_i. In the center of the reduced section the stress rises at 5 μsec intervals to the equilibrium value of 2 σ_i and in section 3 the stress rises at 10 μsec. intervals toward the equilibrium value of σ_i. The duration of each step is governed by the transit time of the wave through the reduced section and the sloping part of each step is of the same duration, namely that of the rise time.

While the example in Fig. 3 pertained to an area discontinuity, a change in material in section 2 would produce similar results because of the change in modulus E and density ρ. Chiddister and Malvern[6] have shown that the effect of a temperature gradient in a uniform bar causes similar stress transients. In all cases the total time required to reach the equilibrium value of stress depends on both the inpedance (ρcA) mismatch and on the length of the discontinuity. In a complex structure subjected to impact the transient stress condition persists for a long time in the long elements while in the short elements the stress reaches equilibrium after a short time interval. Both of these effects must be considered in the design of a dynamic stress testing machine as one wishes to have a constant stress of long duration applied to the specimen but also wants to reach the equilibrium stress distribution in the specimen as quickly as possible.

EFFECT OF PLASTIC DEFORMATION ON WAVE PROPAGATION

The use of Eq. (3) in the previous section implied the assumption that $d\sigma/d\varepsilon = E$ and that E is a constant for a given material. This assumption is valid for crystalline solids where the stretching of the atomic bonds is nearly linear and rate independent. The assumption of constant E for polymers would certainly not be a good one because the complex molecular bonding causes a nonlinear and rate sensitive stress strain relation. Similarly if the stress at any point in a metal exceeds the yield strength, plastic deformation occurs and $d\sigma/d\varepsilon$ is no longer constant. To make use of a unique static stress strain relation in order to determine $(d\sigma/d\varepsilon)_{plastic}$ would a priori assume that no strain rate

(subscript)

effect exists and thus void any experimental strain rate effect determination which requires this assumption in the analysis. But one can approach the problem indirectly, using long elastic members in which the transient stress conditions can be calculated for loading and measuring and very short specimens, where equilibrium can be established very rapidly, to provide the plastic property information.

EXPERIMENTAL TECHNIQUE

Fig. 4 shows three arrangements of a modified split Hopkinson bar for performing compression, double shear and tension tests on any arbitrary material at high strain rates. In each case long elastic input and output rods are used for stress pulse shaping and measuring. On impact of the ram with the input bar a step in stress is propagated down each member. If both the ram and input bar are free of discontinuities, a constant value of stress is obtained whose magnitude depends on the impact velocity and the respective impedances (ρcA) of the members. If the ram should contain a discontinuity such as an attached anvil head, the effect would be similar to the one described in Fig. 3 and a series of steps would result in the stress wave propagated down each bar. These steps would make the plastic analysis of the specimen more difficult. If an anvil is required because of insufficient hardness of the ram, the length of the discontinuity should either be very short so equilibrium is reached quickly or it should be very long so the duration of a single step in stress level is equal to the test duration. The rise time of the stress wave depends on the perfection of alignment between the impact faces of the ram and the input bar. With reasonable constraints a rise time of

2 to 3 μsec. is possible on $\frac{1}{4}$" diameter input bars. For the tension test in Fig. 4, the rise time of the tension stress in the input bar is determined both by the impact of the ram with the transmitter bars and the dimensions of the transfer connection. The stress level in the input bar corresponds to σ_3 and that in the transmitter bar to σ_i in Fig. 3. Again one has the choice of making the connection very short to achieve rapid equilibrium or to make the connection very long and use the first step in stress level for the entire test. Ideally then, one wishes to have an elastic stress wave of constant amplitude and rapid rise time to propagate past the input gage and reach the specimen. Discontinuities or even tapered sections in the input bar may be used if a nonconstant input stress is desired. But even with uniform sections the stress level will fluctuate somewhat because of the transverse stress oscillations in the bars due to the Poisson's expansion. The magnitude of these oscillations can be minimized by using small diameter bars or tubes.

The input gages must provide a measurement of the stress level of the incoming stress wave and the magnitude of the reflected waves from the specimen. The output gage provides a measurement of the transmitted stress. The measurements can be accomplished by either strain gages or velocity gages. Since the behavior in the input and output bars is purely elastic, E is constant and if ρ and c are known for the material, Eq. (3) relates the stress and particle velocity. Velocity transducers which do not require a discontinuity in the bar have been used by Ripperger and Yeakley[7] and Malvern and Efron[8], but these gages are difficult to

construct and calibrate. It is easier to use symmetrically mounted strain gages, wired in such a way as to cancel stresses due to any bending moment present. If subjected to impact, electric strain gages require the use of nonmagnetic gage and rod material to avoid the signal induced by magnetostriction, which would appear as an apparent strain. The gages must be mounted with a thin layer of nonbrittle cement to give a true reading and not break off due to the high shock load. The electrical connections must be made with a minimum of solder and with fine wire or ribbon to reduce the overall mass and thus minimize the load on the cement because the gages are subjected to high accelerations by the passing stress waves. (The particle velocity in the bar may go from zero to about 100 ft/sec in 3 μsec.) Because of the high harmonic content of a sharply rising square wave, the electronic signal amplifiers must have a wide band pass or the filtering action of the circuits removes some of the information required for analysis. For optimum results a band pass of 10 MC or greater is desirable. The amplified input and output signals are displayed on single sweep oscilloscopes and recorded by means of a camera mounted on the scope. The overall experimental arrangement is shown in Fig. 5.

ANALYSIS OF THE MEASUREMENTS

As was shown in Fig. 3, reflections and transient stress waves arise even in a completely elastic specimen. These transients can be accounted for by the use of Equations (5) and (6). But if plastic deformation takes place in the specimen, the transient stress waves will differ from those predicted by the elastic analysis, and it is this difference that contains the information as to the plastic behavior of the specimen. Since the input

and output rods remain in the elastic state at all times, the stress and particle velocity can be determined for section I and II in Fig. 4 at all times. These sections are common to the bars and the specimen and so the stress and particle velocity at each end of the gage section is known. If the specimen is small enough so that the transit time for the elastic wave is short, equilibrium throughout the specimen is rapidly established and plastic deformation takes place uniformly within the specimen. The elastic rods at the ends of the specimen constrain the lateral plastic deformation somewhat due to friction but with a good surface finish on the rods and a light film of lubricant the final shape of the deformed compression specimens shows little barreling below 15% strain. This lateral constraint nevertheless limits the minimum thickness of the specimen.

The mathematical analysis for obtaining the stress, strain, strain rate data has been presented previously[3] but is included here in a more complete form.

In Fig. 4a, on impact of the ram, a compressive stress σ_i propagates down the input bar and is partially reflected on reaching the specimen. This reflected stress σ_r due to the impedance mismatch at the interface I propagates back toward the ram past the input gage. The input gage then records ($\sigma_i - \sigma_r$). At interface I, that part of the input stress which the specimen can support is transmitted as σ_t. As the specimen strain-hardens, higher stress can be supported and σ_t increases while σ_r decreases as a function of time. The transmitted stress σ_t in turn is partially reflected at interface II as σ_r^1 and the stress σ_t^1 is transmitted into the output bar and recorded at the output gage. The reflected

part of σ_t at interface II is reflected back and forth within the specimen and soon reaches the equilibrium distribution (see $\sigma_{(2)}$ in Fig. 3).

Considering the equilibrium of forces at I and II we have

$$\Sigma F_I \rightarrow (\sigma_i - \sigma_r)A_1 = \sigma_t A_2$$

$$\Sigma F_{II} \rightarrow (\sigma_t - \sigma_r^1)A_2 = \sigma_t^1 A_1$$

where all stresses are measured at the same instant of time. The average stress in the specimen is then

$$\sigma_{Avg} = \tfrac{1}{2}(\sigma_I + \sigma_{II})$$

$$\sigma_{Avg} = \frac{\sigma_t + (\sigma_t - \sigma_r^1)}{2} = \frac{(\sigma_i - \sigma_r) + \sigma_t^1}{2}\left(\frac{A_1}{A_2}\right) \qquad (6)$$

where all the stresses are measured at I and II. Actually $(\sigma_i - \sigma_r)$ and σ_t are measured at the gages but they can be phased properly in time to permit calculations of the average stress in the specimen.

The displacements X_I and X_{II} at the input and output ends of the specimen can be computed using Equation (3) and setting the particle velocity v in the bars equal to $\frac{dX}{dt}$.

$$dX = \frac{\sigma}{\rho c}\, dt$$

$$X_I = \frac{1}{\rho c}\int_0^t (\sigma_i - \sigma_r)dt$$

$$\text{and } X_{II} = \frac{1}{\rho c}\int_0^{t^1} \sigma_t^1 dt^1 = \frac{1}{\rho c}\int_{a/c_2}^{t} \sigma_t^1 dt$$

where c_2 is the wave velocity in the specimen and a is the gage length. For very short specimens the lower time limit correction for X_{II} becomes

negligible.

The average strain in the specimen of gage length a will then be

$$\varepsilon_{Avg} = \frac{X_I - X_{II}}{a} = \frac{1}{\rho ca}\left[\int_0^t (\sigma_i - \sigma_r)dt - \int_{a/c_2}^t \sigma_t^1 \, dt\right] \qquad (7)$$

and the average strain rate

$$\dot{\varepsilon}_{Avg} = \frac{d\varepsilon}{dt} = \frac{(\sigma_i - \sigma_r) - \sigma_t^1}{\rho ca} \qquad (8)$$

Fig. 6 shows the procedure for the graphical solution of Equations (7) and (8).

EXAMPLES OF RESULTS

Fig. 7 illustrates the use of equations (4) and (5) to predict the transient stress at station (1) in the elastic bar with a single change in cross section. In the measured record the rise time is about 10 μsec. and the oscillations on the first step are due to lateral vibrations excited by the lateral Poissons expansion. In the fourth step on the stress curve, the first reflection from the free end arrives with the much larger amplitudes of oscillations from the thick section. From that time on there is appreciable deviation of the observed record from the predicted wave shape. Therefore, the one dimensional elastic analysis used is not very accurate when one attempts to predict stress waves in thick sections.

The experimental results of a plastically deforming compression specimen are shown in Fig. 8. The 0.4" long 3/4" diameter tubular Al specimen was held between two hardened Al tubes of the same cross section. The experimental arrangement and analysis are as shown in Fig. 6. The resulting

stresses, strains and strain rates at three points are indicated. Although the example shown in Fig. 8 shows poor alignment and large oscillations, the overall strain measured on the specimen after the experiment was within 5% of the total strain predicted in the analysis.

By performing a series of experiments using different gage length and impact velocities, the constitutive equation curves for the material at a particular temperature can be constructed as shown in Fig. 9. This particular stress, strain, strain rate relation has been used by Rajnak and Hauser[4] to predict the final shape of a long tubular cylinder impacted at one end and free at the other. The final "trumpet" shape of the tube was calculated using the method of characteristics to solve the governing plastic wave propagation equations. Unfortunately, even with the simple boundary conditions in that problem, the solution necessitated the lengthy use of a computer, but the final predicted strain distribution agreed very closely to the measured distribution.

In Fig. 9 it can be seen that almost identical results are obtained for long specimens impacted at high velocities (such as #150) or short specimens at low velocities (#140). At the same strain and strain rate the measured flow stresses are equal indicating the negligible effect that the difference in ratio of end constrained volume to total volume produces.

As an example of a more strain rate sensitive material, the stress, strain, strain rate relation for a type 304 stainless steel are shown in Fig. 10. Here the static tests are also included showing the effect of changing the strain rates by seven orders of magnitude. The maximum strain rate attained in these tests was limited by the maximum velocity of the

impact ram (1000 inch/sec.). The Ti input and output bars used in this test have a yield strength of 150 ksi and this strength would impose a new upper stress limit if a higher velocity impact source were available.

The final example shows the experimental records obtained when testing a brittle material. Gabbro rock, which normally crumbles at a compressive stress of about 30 ksi, withstood over 65 ksi for about 3 μsec. when loaded rapidly as shown in Fig. 11. The dip in the input bar stress at 40 μsec. corresponds to the elastic compression of the rock while the dip at about 47 μsec. in both records corresponds to the stepwise crumbling of the material. Other tests on single crystals of MgO show steps on the rising part of the output bar stress, indicating some possible local yielding or cracking before final failure. Similarly to the delay time for crumbling measured in Fig. 11, the delay time for onset of plastic deformation in steels can be measured by the same method.

LIMITATIONS OF THE TESTER

The test equipment described permits the determination of the stress, strain, strain rate relation of many materials in the range from 100 per sec. to about 100,000 per sec. However there are certain limitations inherent in the method. As the analysis assumes equilibrium conditions in the sample being deformed, and this condition does not exist during the first few μseconds of the test, the data obtained at very low strain values are not reliable. Proper design of the equipment helps, but the problem can only be minimized and not eliminated. The upper limit of strain rate and stress are determined by the yield strength of the input bar. If plastic deformation takes place in this bar, the analysis as

described no longer applies, as the position of the interface between specimen and bar can no longer be determined by the elastic equation (3). Finally, the operation of the tester and the interpretation of the records requires a thorough understanding of the mechanical and electrical systems involved. This unfortunately prevents the procedure from becoming a simple routine test. But as a research tool, the tester operated by many different students at the University of California has yielded heretofore unavailable high strain rate information and this data has been of great help in research on basic deformation and fracture mechanisms.

* * *

ACKNOWLEDGMENTS

The author wishes to express his appreciation to the Convair Division of General Dynamics Corporation and to the Inorganic Materials Research Division of the Lawrence Radiation Laboratory for support and sponsorship of the research. He also wishes to thank Mr. C. A. Winter for help in the design of the tester and to Professor J. E. Dorn for his continued interest and suggestions.

FEH:sw
5/3/65

BIBLIOGRAPHY

1. V. M. Krafft, "Instrumentation for High-Speed Strain Measurements," in Response of Metals to High Velocity Deformation, Interscience, New York, 1961, p. 9.

2. H. Kolsky, Stress Waves in Solids, Oxford University Press, London, 1953.

3. F. E. Hauser, J. A. Simmons and J. E. Dorn, "Strain Rate Effects in Plastic Wave Propagation," in Response of Metals to High Velocity Deformation, Interscience, New York, 1961, p. 93.

4. S. L. Rajnak and F. E. Hauser, "Plastic Wave Propagation in Rods," in Symposium on Dynamic Behavior of Materials, A.S.T.M. Special Pub. No. 336, 1962, p. 167.

5. T. L. Larsen, S. L. Rajnak, F. E. Hauser and J. E. Dorn, "Plastic Stress/Strain Rate/Temperature Relations in H.C.P. Ag-Al Under Impact Loading," J. Mech. Phys. Solids, Vol. 12, 1964, p. 361.

6. J. L. Chiddister and L. E. Malvern, "Compression-Impact Testing of Al at Elevated Temperatures," Experimental Mechanics, Vol. 3, April 1963, p. 81.

7. E. A. Ripperger and L. M. Yeakley, "Measurement of Particle Velocities Associated with Waves Propagating in Bars," Experimental Mechanics, Vol. 3, February 1963, p. 47.

8. L. E. Malvern and L. Efron, "Longitudinal Plastic Wave Propagation in Annealed Aluminum Bars," Tech. Report No. 1, NSF Grant G-24898, Michigan State University, 1964.

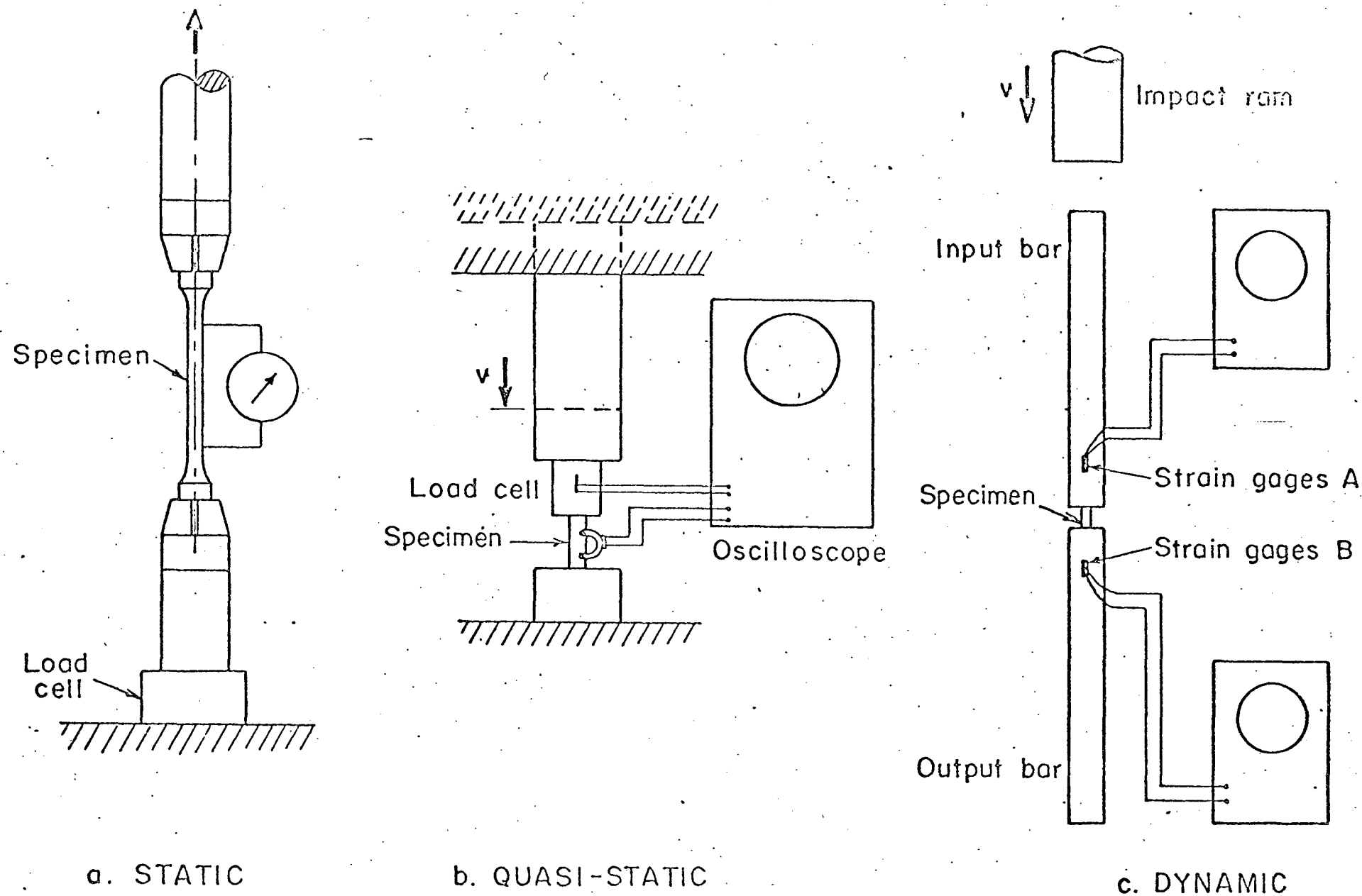

FIG. 1 THREE POSSIBLE MATERIAL TEST ARRANGEMENTS.

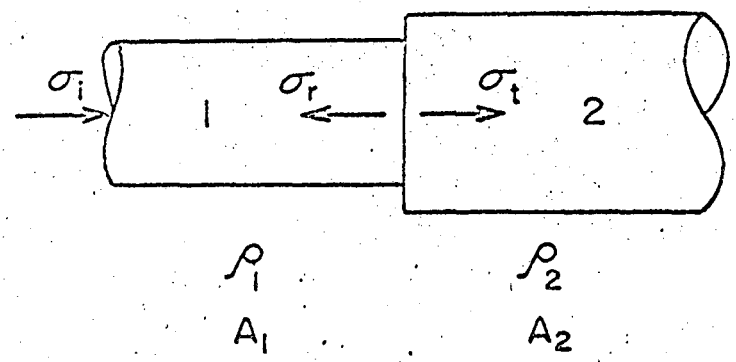

ρ = mass density

At the interface,

$\Sigma F = 0$; $\quad (\vec{\sigma}_i + \overleftarrow{\sigma}_r) A_1 = \vec{\sigma}_t A_2$ ---------- (1)

Continuity $\quad v_1 = v_2$; $\quad v_i - v_r = v_t$ ---------- (2)

$\sigma = \rho c v$, ---------- (3)

for elastic wave propagating with velocity $c = \sqrt{E/\rho}$

Combine to get;

$$\overleftarrow{\sigma}_r = \frac{\rho_2 c_2 A_2 - \rho_1 c_1 A_1}{\rho_2 c_2 A_2 + \rho_1 c_1 A_1} \vec{\sigma}_i \quad \text{-------(4)}$$

$$\vec{\sigma}_t = \frac{2 \rho_2 c_2 A_1}{\rho_2 c_2 A_2 + \rho_1 c_1 A_1} \vec{\sigma}_i \quad \text{-------(5)}$$

FIG. 2 ELASTIC WAVE PROPAGATION.

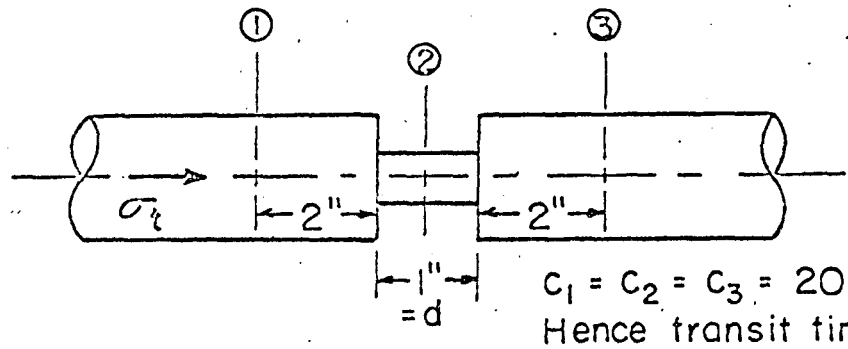

$c_1 = c_2 = c_3 = 200{,}000$ in/sec.
Hence transit time = 5 μ secs.

Let $A_1 = A_3 = 2A_2$; $\rho_1 = \rho_2 = \rho_3$

Then ① → ② $\vec{\sigma}_t = 4/3\,\sigma_i$ and $\overleftarrow{\sigma}_r = -1/3\,\sigma_i$

so $\sigma_{①} = 2/3\,\sigma_i$, $\sigma_{②} = 4/3\,\sigma_i$

② → ③ $\vec{\sigma}_t' = 2/3\,\sigma_{②}$ and $\overleftarrow{\sigma}_r' = 1/3\,\sigma_{②}$

so $\sigma_{③} = 8/9\,\sigma_i$, $\sigma_{②} = 16/9\,\sigma_i$

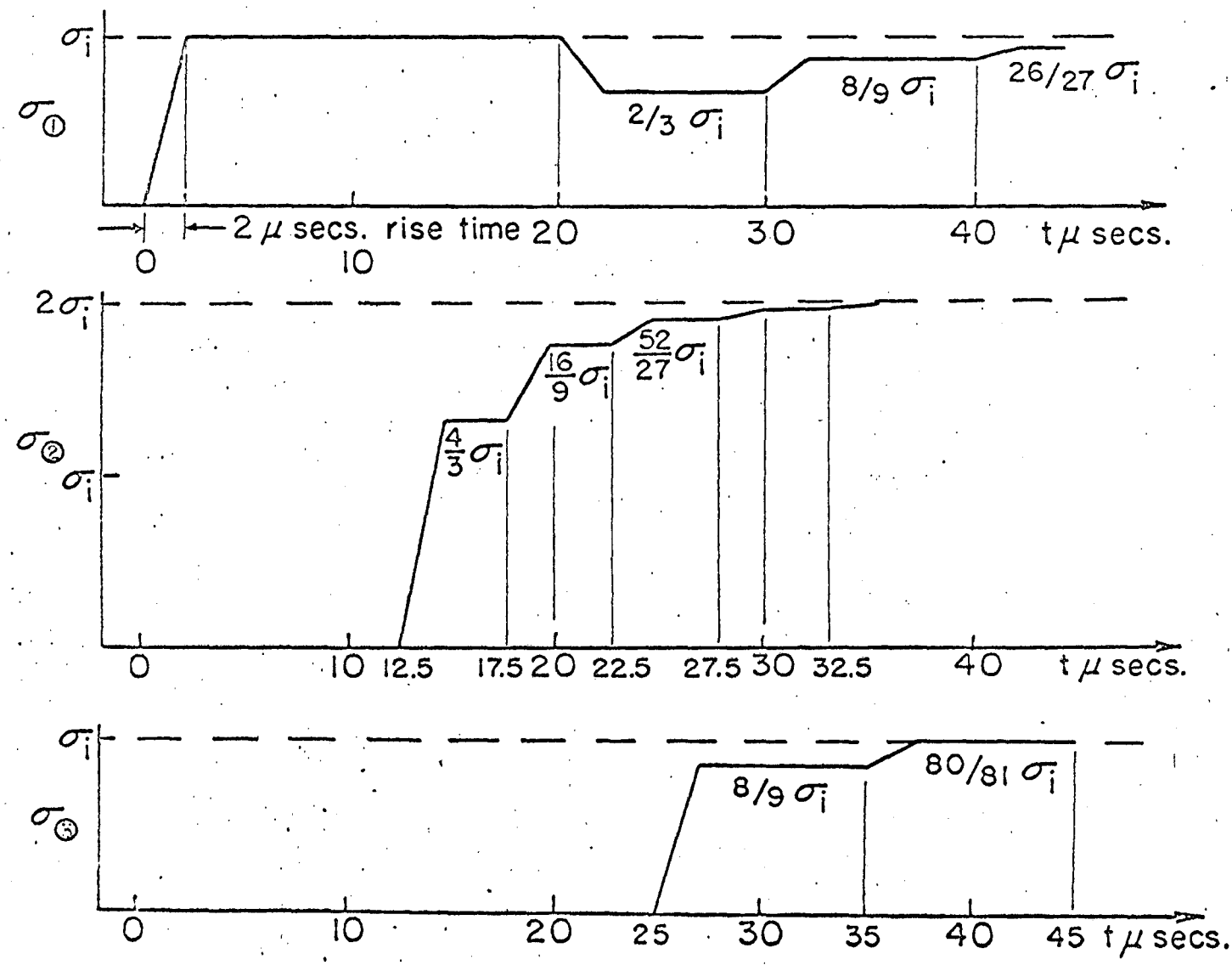

FIG. 3 EXAMPLE OF ELASTIC WAVE PROPAGATION.

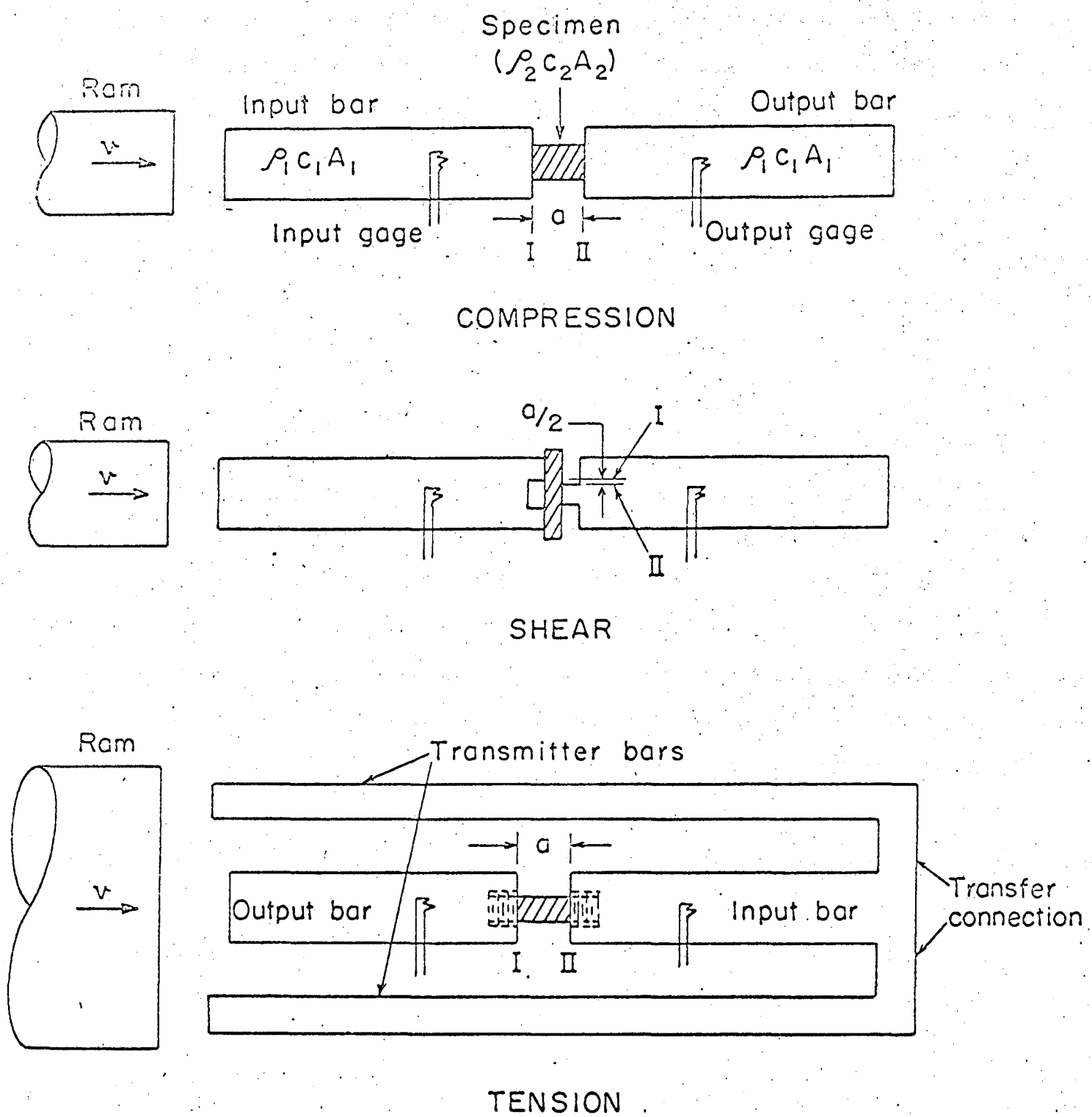

FIG. 4 EXAMPLES OF COMPRESSION, SHEAR AND TENSION TEST ARRANGEMENTS.

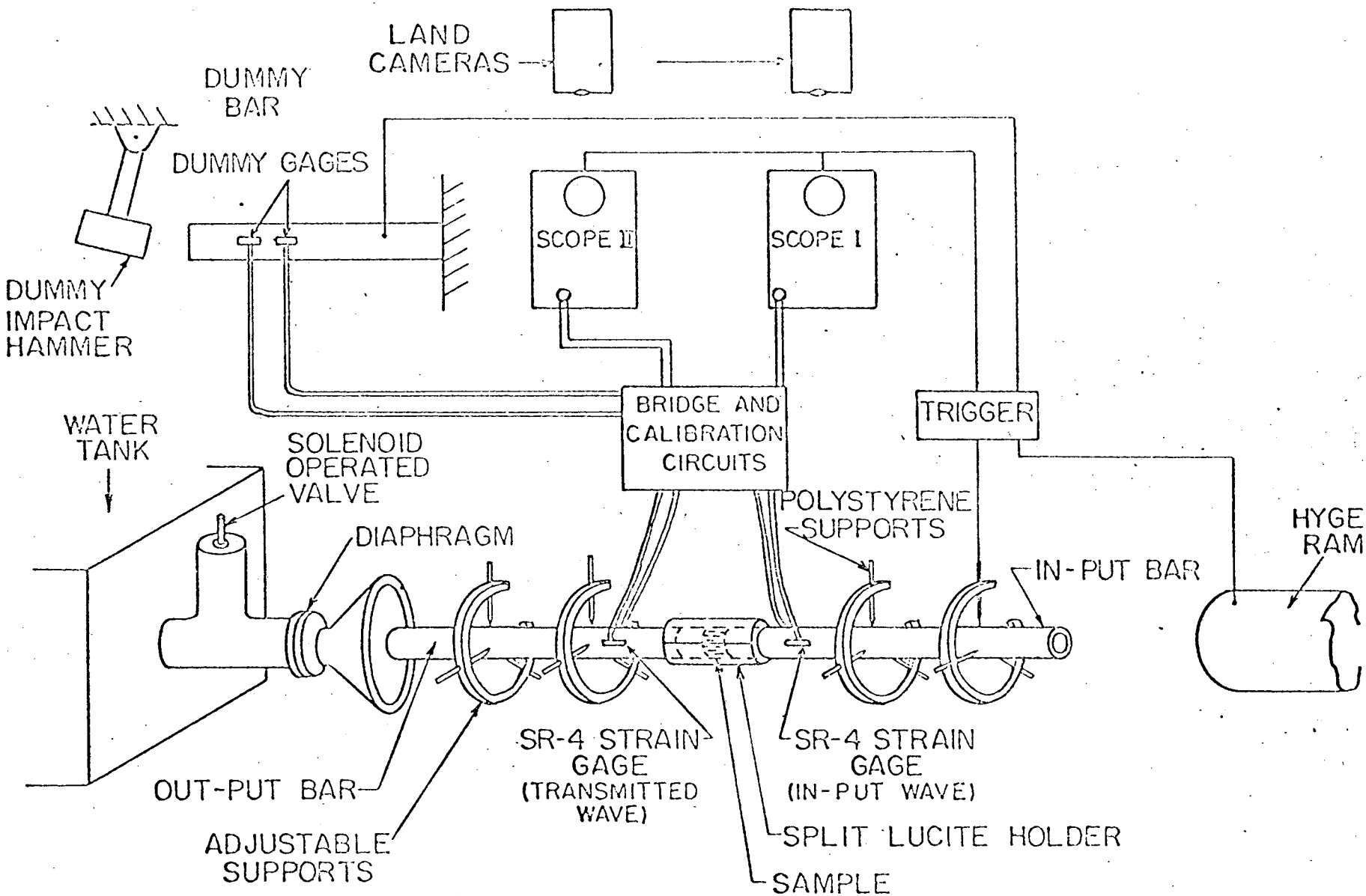

FIG. 5 EXPERIMENTAL ARRANGEMENT AND INSTRUMENTATION.

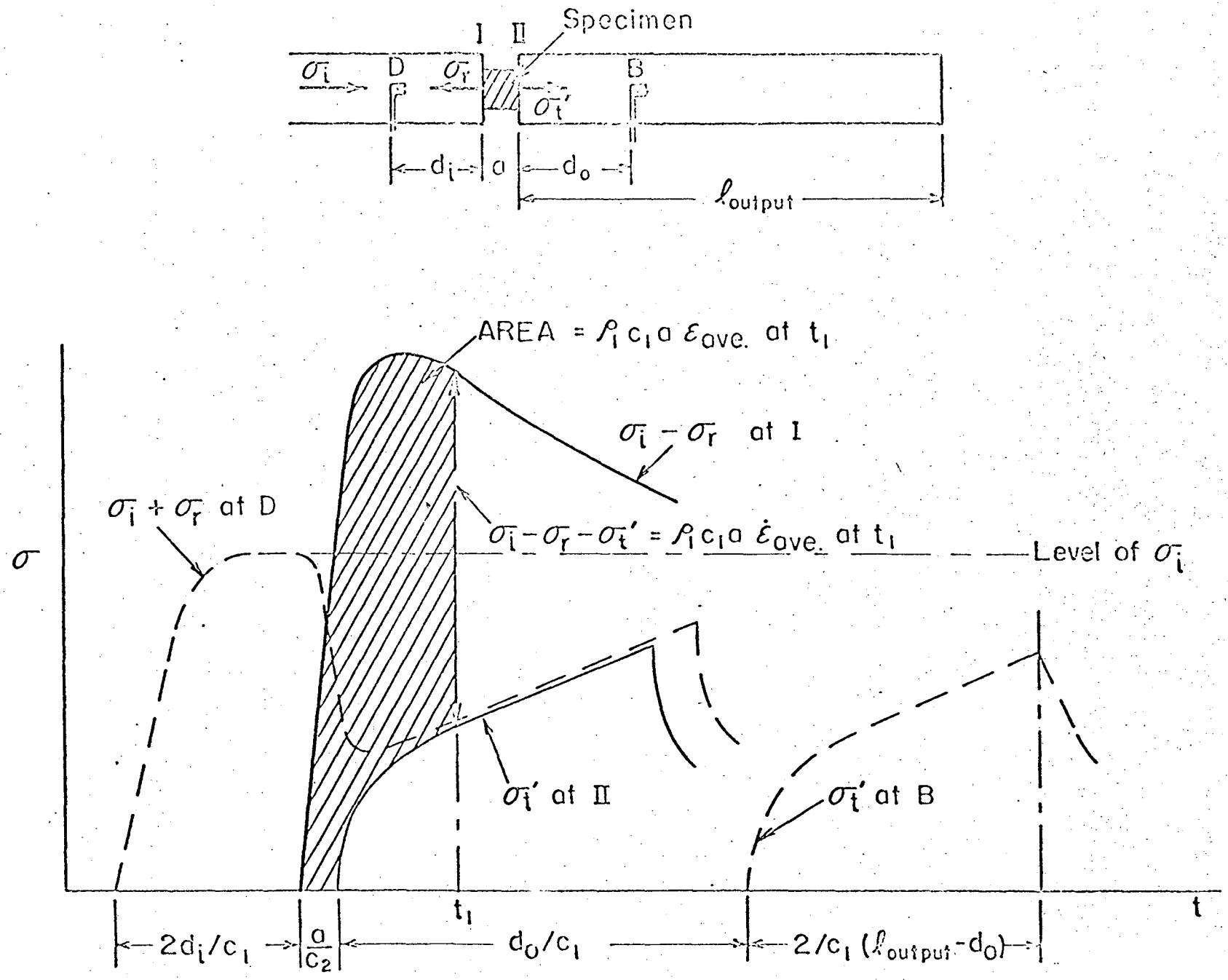

FIG. 6 GRAPHICAL SOLUTION TO EQUATIONS (7) AND (8).

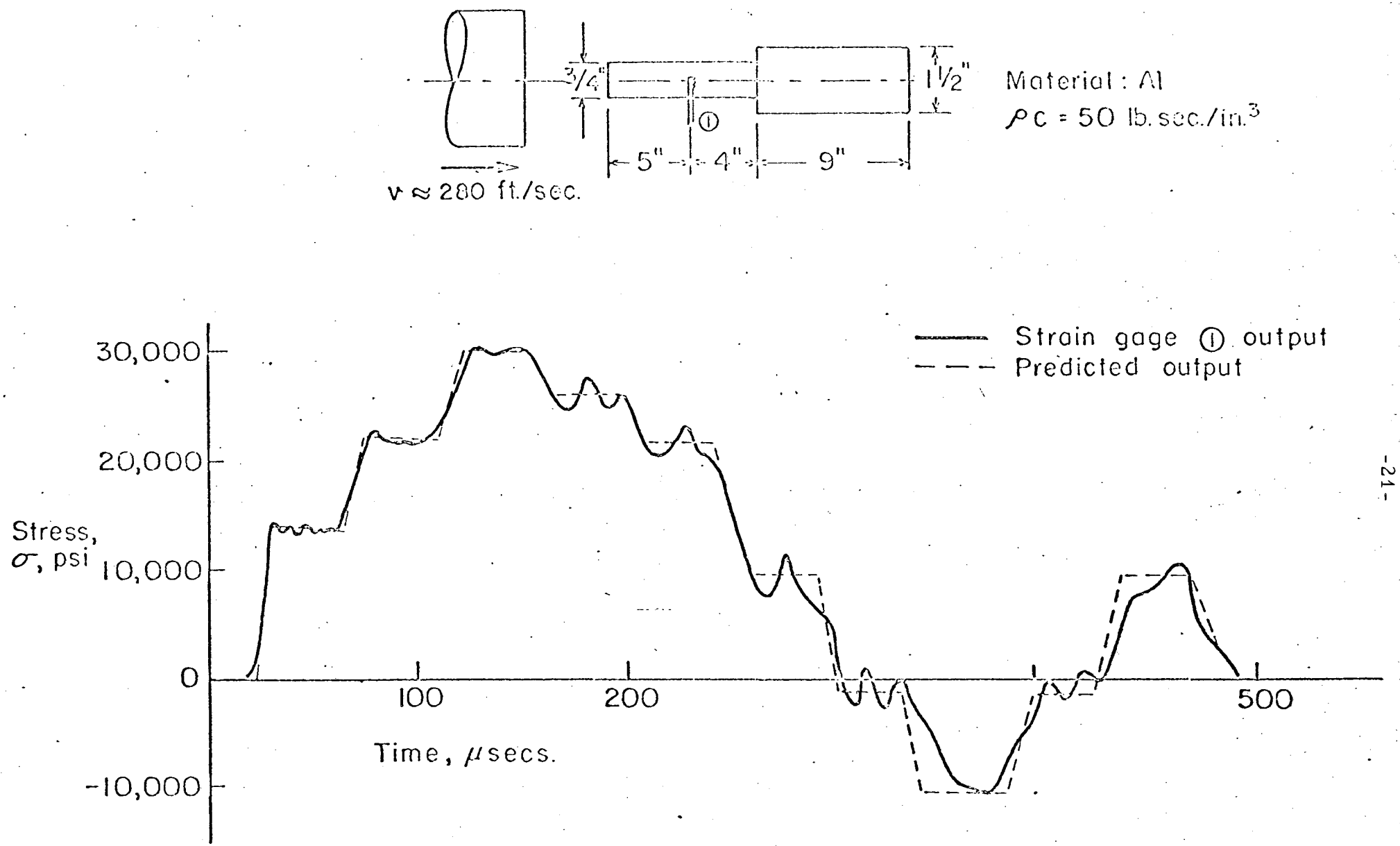

FIG. 7 TRANSIENT ELASTIC STRESS DISTRIBUTION IN A STEPPED BAR.

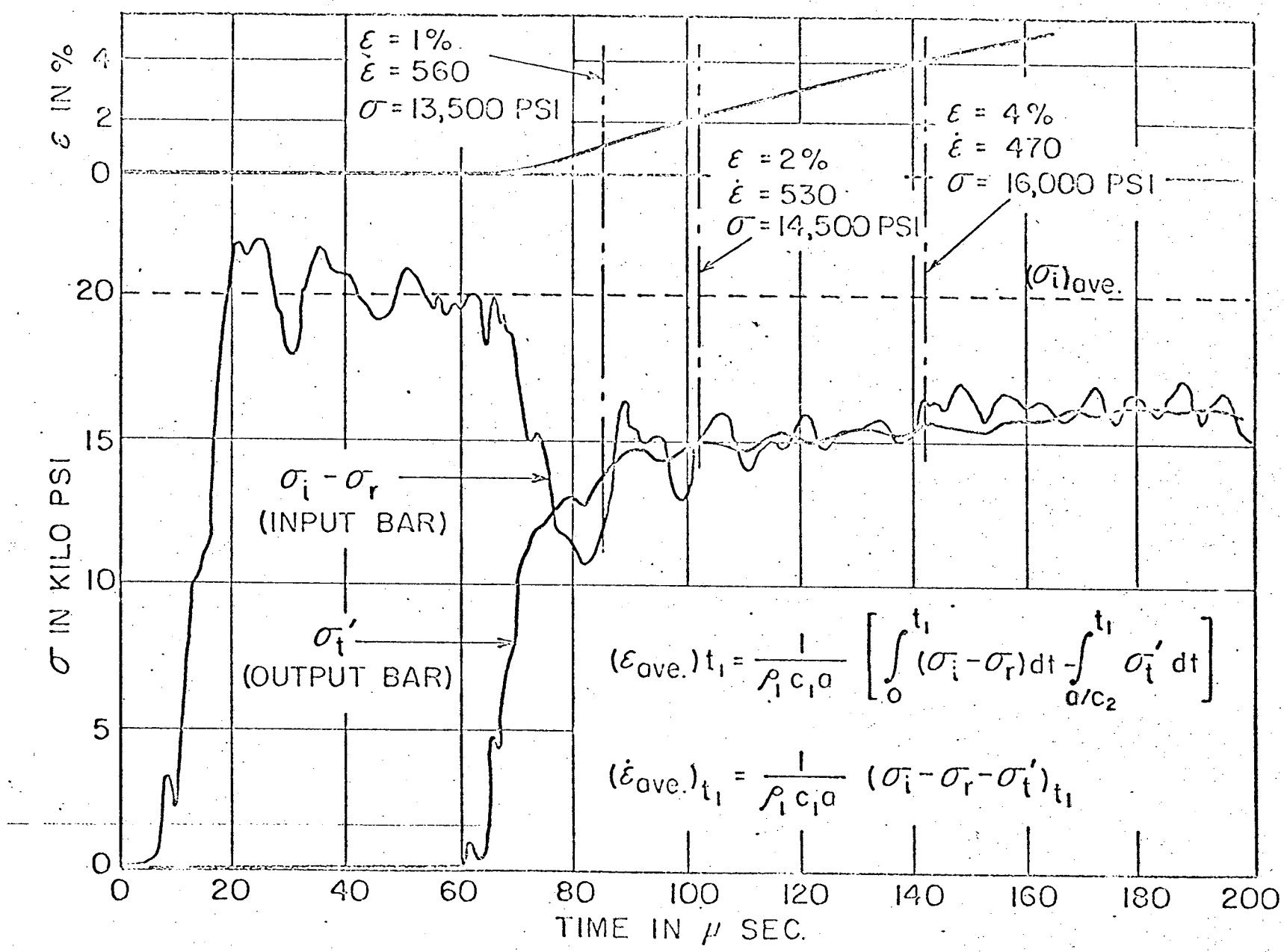

FIG. 8 EXPERIMENTAL RECORD AND ANALYSIS FOR 0.4" TUBULAR AL SPECIMEN WITH AN APPLIED STRESS OF 20,000 PSI.

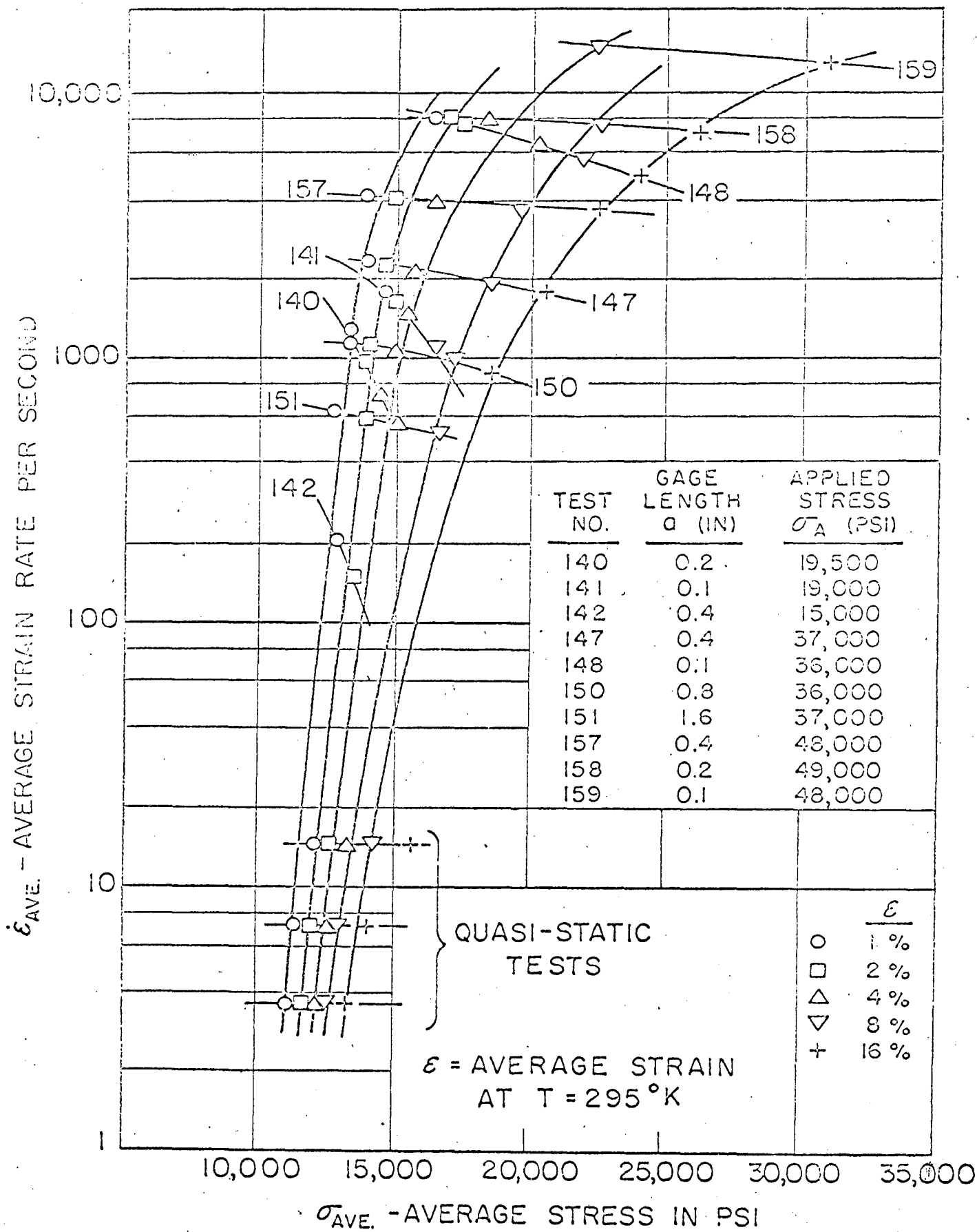

TEST NO.	GAGE LENGTH a (IN)	APPLIED STRESS σ_A (PSI)
140	0.2	19,500
141	0.1	19,000
142	0.4	15,000
147	0.4	37,000
148	0.1	36,000
150	0.8	36,000
151	1.6	37,000
157	0.4	48,000
158	0.2	49,000
159	0.1	48,000

FIG. 9 EFFECT OF STRESS ON STRAIN RATE IN WORK-HARDENED AL. AT CONSTANT STRAIN, SHOWING SAMPLING

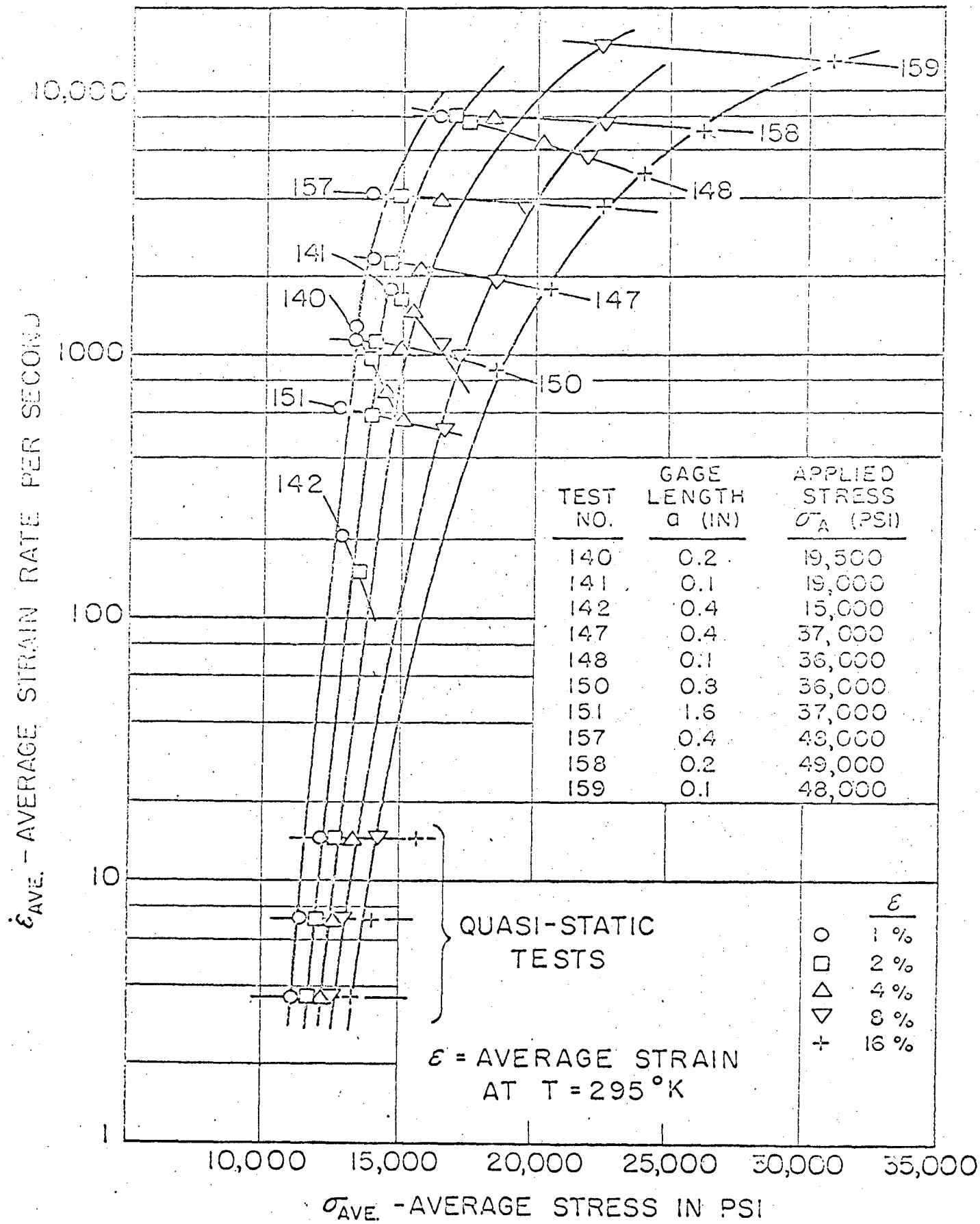

TEST NO.	GAGE LENGTH a (IN)	APPLIED STRESS σ_A (PSI)
140	0.2	19,500
141	0.1	19,000
142	0.4	15,000
147	0.4	37,000
148	0.1	36,000
150	0.8	36,000
151	1.6	37,000
157	0.4	48,000
158	0.2	49,000
159	0.1	48,000

FIG. 9 EFFECT OF STRESS ON STRAIN RATE IN WORK-HARDENED AL AT CONSTANT STRAIN, SHOWING SAMPLING

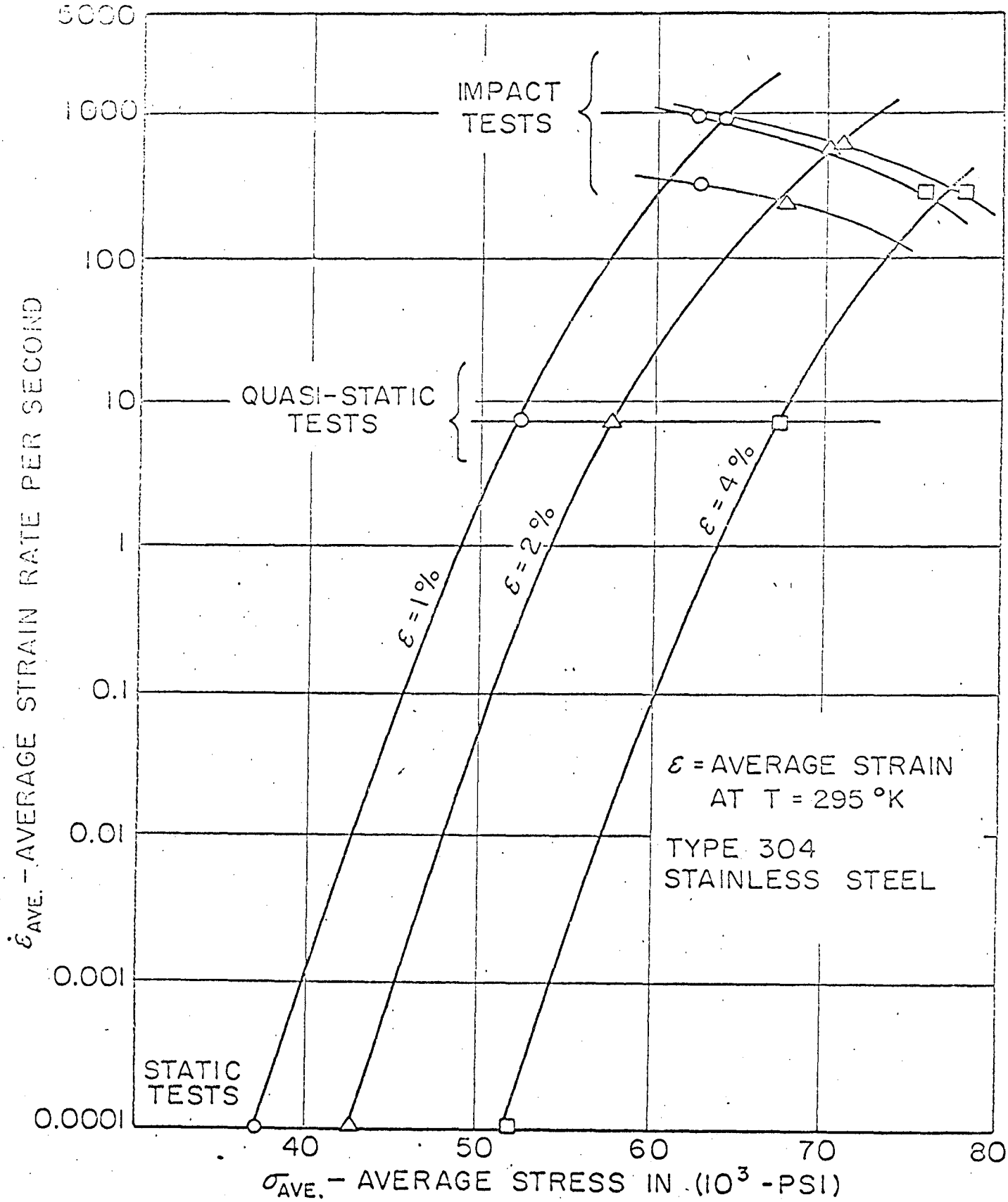

FIG. 10 EFFECT OF STRESS ON STRAIN RATE AT CONSTANT STRAIN FOR STAINLESS STEEL, SHOWING SAMPLING OF EXPERIMENTAL RECORD

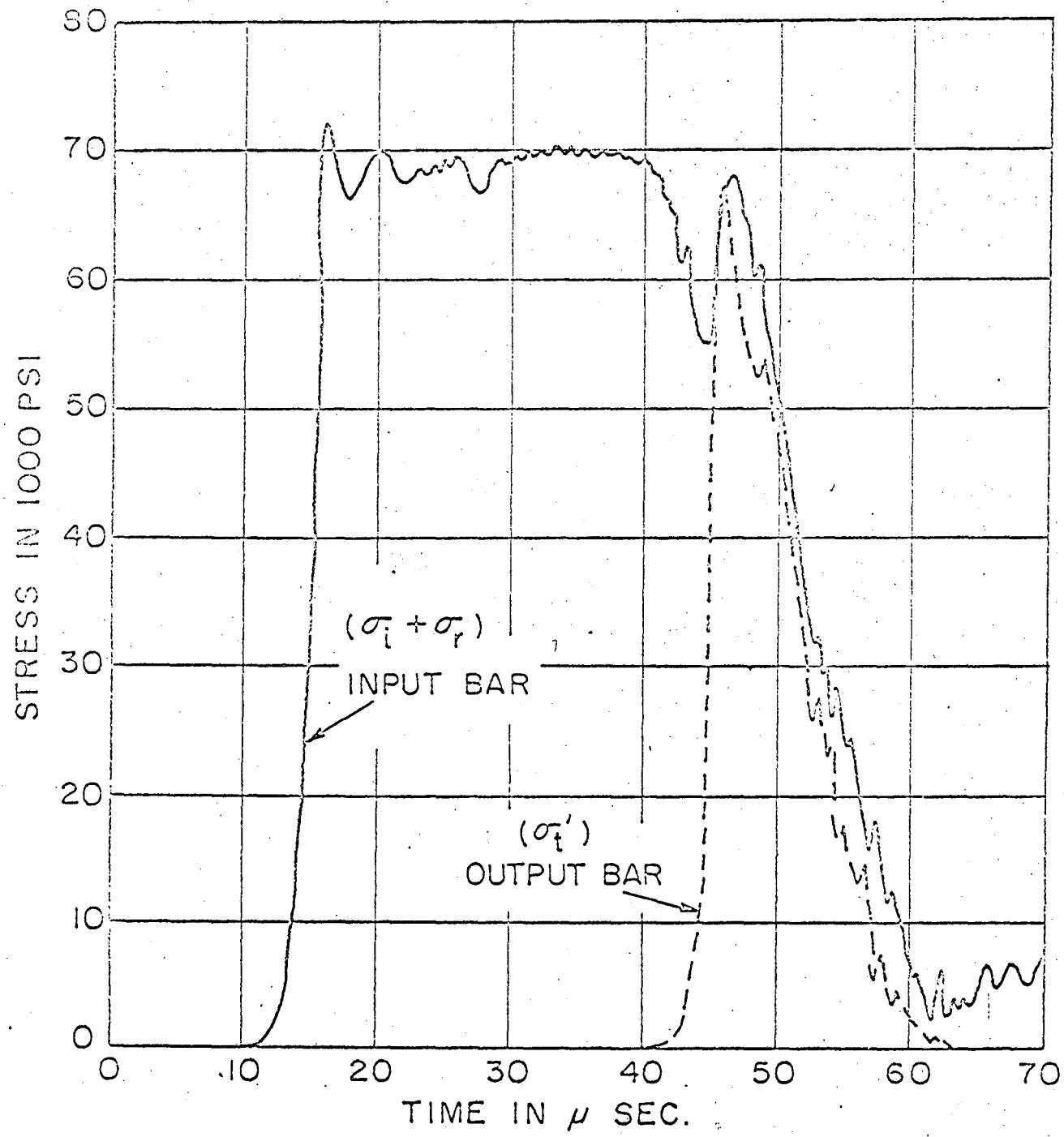

FIG. 11 EXPERIMENTAL RECORD FOR 3/4" LONG GABRO ROCK (STATIC YIELD STRENGTH = 30,000 PSI).